The Astrophysical Journal Letters, 749:L2 (6pp), 2012 April 10 doi:10.1088/2041-8205/749/1/L2

CANDIDATES OF Hα EMITTING REGIONS IN THE MAGELLANIC STREAM IV CLOUD

Masafumi Yagi[1], Yutaka Komiyama[1], and Michitoshi Yoshida[2]
[1] Optical and Infrared Astronomy Division, National Astronomical Observatory of Japan, 2-21-1 Osawa, Mitaka, Tokyo 181-8588, Japan; YAGI.Masafumi@nao.ac.jp
[2] Hiroshima Astrophysical Science Center, Hiroshima University, 1-3-1 Kagamiyama, Higashi-Hiroshima, Hiroshima 739-8526, Japan
Received 2011 October 30; accepted 2012 March 1; published 2012 March 20

ABSTRACT

From Hα narrowband observations, we identified three Hα emitting regions in the direction of Magellanic Stream IV (MS IV). They consist of three parallel filaments of 2 arcmin width and 6–30 arcmin length at 12 arcmin intervals. Their mean surface brightness (SB) is $\sim 2 \times 10^{-18}$ erg s^{-1} cm^{-2} arcsec^{-2}. Because of their low SB, the regions were not detected in previous Hα surveys. In the H I map, the position of the filaments overlap MS, suggesting that they are parts of the MS, but there also exists a local H I structure. If the filaments are associated with the MS, the sizes are 30 pc × 100–500 pc. The filaments lie at the leading edge of a downstream cloud, which supports shock heating and its propagation (shock cascade) model for the ionizing source. If they are local objects, on the other hand, Fossil Strömgren Trails of more than two stars is a possible interpretation, and the sizes would be 0.1 pc × 0.3–1.5 pc at 180 pc distance. The positional information of the Hα filaments presented in this Letter enables future spectroscopic observations to clarify their nature.

Key words: galaxies: individual (Magellanic Stream) – Galaxy: halo – intergalactic medium

Online-only material: color figures

1. INTRODUCTION

The Magellanic Stream (MS hereafter) was found as a long filament of H I gas around our Galaxy (Mathewson et al. 1974). MS is thought to be stripped gas from the Small Magellanic Cloud and/or Large Magellanic Cloud. It has been revealed that the MS consists of multi-phase gas components: molecular gas, H I gas, H II gas, and highly ionized plasma (Fox et al. 2010 and references therein). The MS is the only clear example of a gaseous halo stream in close proximity to the Milky Way (Stanimirorović et al. 2008). It gives us important clues to the physical interaction between the Galaxy and its satellites in detail.

The Hα emission from the MS has been first reported by Weiner & Williams (1996, hereafter WW96). Putman et al. (2003a) have found several other Hα emitting regions. The ionizing source of these regions is still a mystery because no ionizing star is observed in the stream. There are several models to explain the origin of the MS Hα clouds. WW96 argued that the emissions are explained by ram pressure heating. However, this model required a much higher density of halo gas than WW96 estimated because the distance to the MS was found to be larger than expected (Weiner et al. 2001). Bland-Hawthorn & Maloney (1999) presented another model where ionizing photons escaping from the Galactic disk heat up the MS. This model predicted that the Hα emission would be smoothly distributed. However, it is inconsistent with the fact that the contrast of the Hα emission is as large as a factor of 30 (Weiner et al. 2001). Bland-Hawthorn et al. (2007, hereafter B07) presented yet another model incorporating shock heating and its propagation (shock cascade). They predicted a high Hα/Hβ ratio and strong [O II], [S II] emissions, which have not been examined yet. Recently, Fox et al. (2010) investigated the absorption features of active galactic nuclei behind the MS in order to study the ionization structure of the MS Hα clouds. They found that the ionization structure cannot be reproduced by evaporative interaction with the Galactic corona plus photoionization.

In order to study the ionization mechanism and kinematics of the MS Hα clouds, detailed spectroscopic follow-up observations are required. However, positional information necessary to perform medium to high dispersion spectroscopy has been so far very limited. The exact position and detailed morphology of the Hα emitting region found by WW96 were not clear, because they used a Fabry–Pérot interferometer and the spatial structure inside the Fabry–Pérot beam of 7 arcmin diameter was averaged.

There are several other Hα surveys that overlap the MS fields. The Southern Hα Sky Survey Atlas[3] (SHASSA; Gaustad et al. 2001) presents a Hα map of 0.8 arcmin pixel and used a 3.2 nm width filter to detect Hα emissions. The Wisconsin Hα mapper[4] (WHAM; Raynolds et al. 1998; Haffner et al. 2003) provides another Hα map with high velocity resolution in the velocity range from −80 km s^{-1} to +80 km s^{-1} with respect to the local standard of rest (LSR) with a 1° beam using a Fabry–Pérot spectrometer. The spatial resolutions of those works are still not enough for slit spectroscopy.

We performed imaging observations with higher spatial resolution at the northern part of MS IV where WW96 detected the Hα emissions. In this Letter, we report the positions and shapes of the Hα emitting regions we detected.

2. OBSERVATION

We observed two WW96 fields, MS IV-C (23:44:34.8, −12:23:20, J2000.0) and MS IV-D (23:40:49.0,−10:45:32, J2000.0) with the 2kCCD camera (Itoh et al. 2001) mounted on the Kiso 105 cm Schmidt camera at the Kiso Observatory in 2011 September. The pixel scale is 1.5 arcsec pixel^{-1}, and the field of view (FoV) is 51.2 arcmin^2. We used the *R*-band and three narrowband filters (N657, Ha6577, and Ha6417). The filter characteristics are shown in Table 1. The variation of the wavelength coverage is no worse than 3.6 Å across the filter

[3] http://amundsen.swarthmore.edu/
[4] http://www.astro.wisc.edu/wham/

Table 1
Filters Used and 1σ Surface Brightness (SB) of the MS IV-D Field

Filter	Center	FWHM	v (Hα)	1σ SB
R	6475 Å	1450 Å	...	27.4 mag arcsec^{-2}
N657	6577 Å	40 Å	-265...+1563 km s^{-1}	27.3 mag arcsec^{-2} = 210 mR
Ha6577	6577 Å	85 Å	-1294...+2592 km s^{-1}	27.2 mag arcsec^{-2} = 500 mR
Ha6417	6417 Å	85 Å	-8608...-4722 km s^{-1}	26.8 mag arcsec^{-2}

Notes. The column v (Hα) shows the recession velocity coverage for Hα. The 1σ SB is estimated around the highest flux in Figure 1(c) and measured in 15 arcsec^2. For N657 and Ha6577, the SB is also given in units of milli-Rayleigh (mR).

in Ha6577 and Ha6417. For N657, the transmission curve at the corner is shifted by 10 Å to the red from that at the center. We took the exposures with ~ 7.5 arcmin dithering. The typical seeing size was 4.1 arcsec.

The data reduction was performed using the mosaic CCD data reduction packages (Yagi et al. 2002). Overscan subtraction, bias pattern subtraction, and flat fielding with domeflat were performed in a standard manner. The pixel scale of the images are slightly different among filters. The difference was corrected before co-adding using the results by the SMOKA team (S. Ichikawa 2011, private communication).[5] The sky background was subtracted in each frame before co-adding with a background mesh size of 1024 pixels (25.6 arcmin). Therefore, structures larger than 25 arcmin^2 would have been removed. After the co-adding, stellar objects were detected by SExtractor (Bertin & Arnouts 1996), and the astrometric calibration was performed using wcstools (Mink 2002) referring to the USNO-B1 catalog (Monet et al. 2003).

We calibrated the flux using the photometry of stars by Sloan Digital Sky Survey (SDSS) data release 7 (Abazajian et al. 2009) in the northern half of the MS IV-D field. The color conversion from SDSS r and i to Kiso 2kCCD filters is constructed by fitting a quadratic function to the photometry of model spectral energy distributions from the Bruzual–Pearson–Gunn–Stryker atlas[6] and the filter responses, as the method in the Appendix of Yagi et al. (2010). The best-fit functions are

$$\mathrm{Kiso} = r + c_0 + c_1(r-i) + c_2(r-i)^2, \quad (1)$$

where $(c_0, c_1, c_2) = (0.003,\ 0.267,\ 0.052)$, $(-0.075,\ 0.773,\ -0.292)$, $(-0.034,\ 0.653,\ -0.210)$, and $(0.014,\ 0.262,\ 0)$ for R, N657, Ha6577, and Ha6417, respectively, in AB magnitude for $-0.1 < r-i < 1.0$ stars. The dispersion of our photometry around the fit is 0.06–0.1 mag in rms converted from the median of absolute deviation in each band. As MS IV-C is not covered by SDSS, we roughly estimated the zero point using R-band (R_F-band) photometry of USNO-B1.0 (Monet et al. 2003) in the Naval Observatory Merged Astrometric Dataset (Zacharias et al. 2005). The error is estimated to be ~ 0.15 mag. Galactic extinction is about $A_R = 0.08$–0.09 in MS IV-C and MS IV-D from Schlegel et al. (1998) via the extinction calculator in the NASA/IPAC extragalactic database (NED).[7] We adopted 0.09 mag for all of the four bands. The limiting surface brightness (SB) of the final images of MS IV-D in 15×15 arcsec^2 (10×10 pixel^2) is presented in Table 1.

3. DETECTION OF THREE Hα EMITTING REGIONS

We performed eye inspections to detect possible Hα emitting regions. In the MS IV-C field, we could not find any sign of Hα excess brighter than 800 mR[8] with size between 15 arcsec and 25 arcmin scale in the 54×54 arcmin^2 field. The conversion from SB of N657–R to total Hα+[N II] brightness requires the redshift and the line full width at half-maximum (FWHM) information, which are still unavailable. In this study, we therefore assume that the line is located at the wavelength of the maximum transmittance of each filter, and that the line width is much narrower than the filter FWHM. This gives the lower limit of the Hα+[N II] brightness.

In the MS IV-D field, we detected regions with N657 excess relative to the R band. Figures 1(a) and (b) show the R-band subtracted N657 image (N657–R image) and the N657 image of the MS IV-D field, respectively. The images were binned by 10×10 pixels (15 arcsec square) to increase the signal-to-noise ratio (S/N). Three filamentary Hα regions are seen in the lower half region of Figures 1(a) and (b). We call the Hα regions D1, D2, and D3 from east to the west hereafter. Except for these three, we could not detect Hα emitting structures brighter than 240 mR (1σ of the N657–R image) with size between 15 arcsec and 25 arcmin scale in the 74×60 arcmin field of MV IV-D. Figure 1(c) shows the effective exposure time map of N657-R and the position of the Hα regions. Because of the bad weather, the southwest part has low S/N. It should also be noted that a bright star at the southwest of D2 made it difficult to measure the emission around it.

We found D1 and part of D3 in the Ha6577 image with an SB of 26.3 mag arcsec^{-2}. The three Hα regions are fainter than 27 mag arcsec^{-2} in the R band. In the Ha6417 image, neither D1 nor D2 were detected, and D3 was located outside of the FoV. D1 was also found in the N657–Ha6417 image, and marginally recognized in the Ha6577–Ha6417 image. In the Ha6577–R image, D1 and D3 were detected, and D2 was marginally detected. In the N657–Ha6577 image, D1 was marginally positive (N657 bright) with low S/N, and D2 and D3 were not detected. In summary, excess was found in N657–R, N657–Ha6417, and Ha6577–R, and marginally in N657–Ha6577. The detection in several combinations of bands suggests that the features are real emissions.

We investigated the possibility of artifacts. If the filaments were fringes made by sky lines, they should also appear in other fields, but we could not detect such features in other fields (e.g., MS IV-C). We also checked whether the regions were seen in co-added images of each day and confirmed that they were neither moving objects nor transient phenomena. The positions and

[5] http://smoka.nao.ac.jp/about/KCD_astrometric_calib.jsp
[6] ftp://ftp.stsci.edu/cdbs/grid/bpgs/
[7] http://ned.ipac.caltech.edu/forms/calculator.html

[8] 1 Rayleigh (1 R) is 10^{10} photons m^{-2} s^{-1} str^{-1}, which corresponds to 5.66×10^{-18} erg s^{-1} cm^{-2} arcsec^{-2} at 6563 Å, and 1 R=1000 mR.

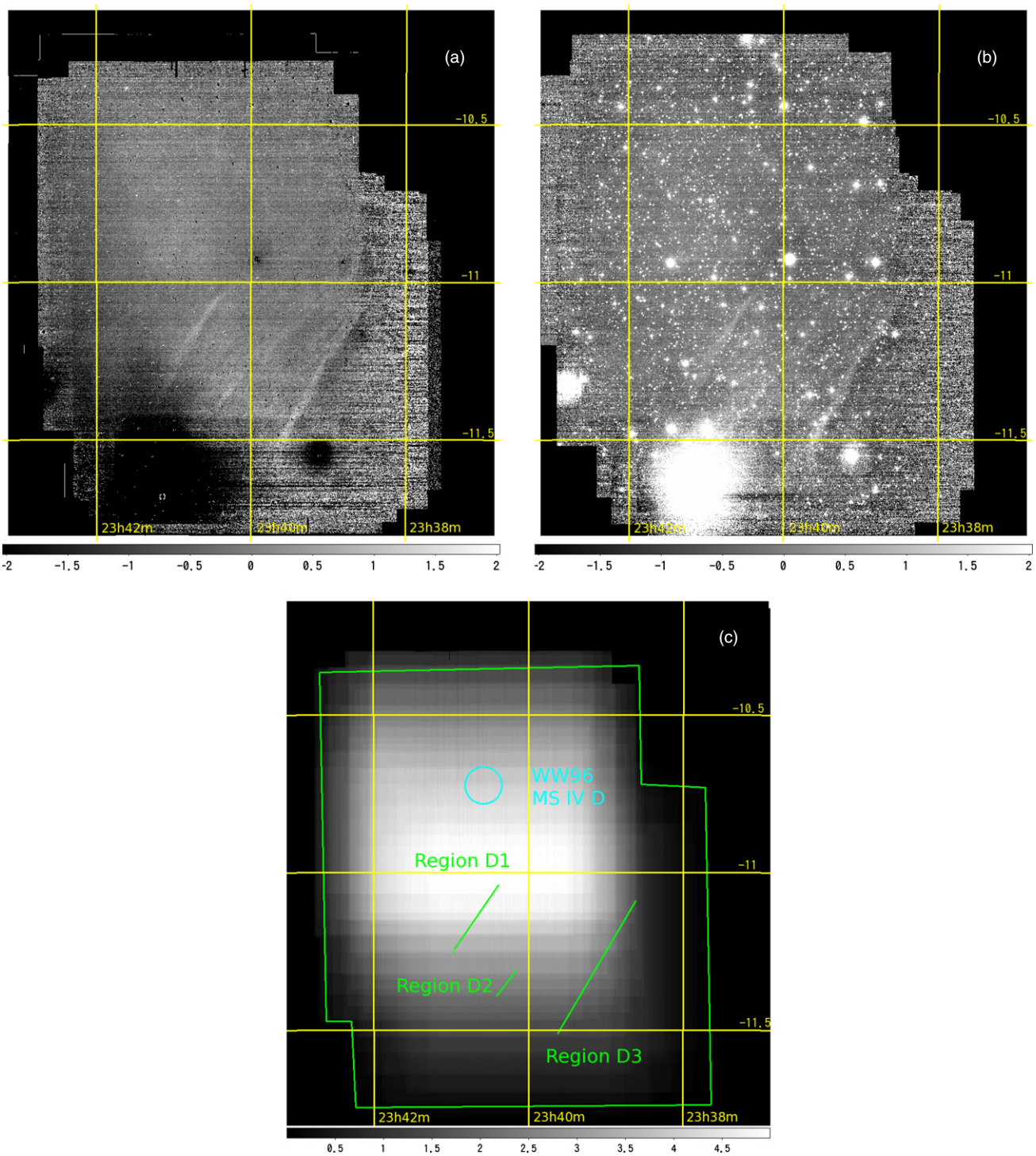

Figure 1. Co-added images of the MS IV-D field: (a) N657-R and (b) N657. North is up, and east to the left, and the coordinates are J2000.0. The image size is 87.5 × 100 arcmin. The scale of color bar is in units of Rayleighs. Effective exposure time map of N657-R is shown in (c). The color bar is in units of hours. The aperture of WW96 (cyan) and the position of the Hα emitting regions (green) are overlaid.

(A color version of this figure is available in the online journal.)

the shapes remained the same during the observation. When we observed other brighter stars in another field, we found that some ghosts of the optics appear. The ghosts moved when we shifted the FoV, and they appeared at different positions in Ha6577 and N657. On the contrary, D1–D3 did not move and stayed at the same position in the sky in both filters. Moreover, we made additional observations in 2011 November for the filaments with Ha6577. At that time, we shifted the field to avoid the bright star at the southeast. The filaments D1 and D3 were still detected at the same position. D1–D3 are therefore not ghosts. We conclude that the three regions are genuine Hα emitting regions.

The flux-weighted center of the regions is shown in Table 2. The positions are 20–50 arcmin away from the aperture of MV IV-D by WW96 (Figure 1(c)).

We defined the boundary of the filaments for a quantitative analysis as follows. First, we masked bright objects in the

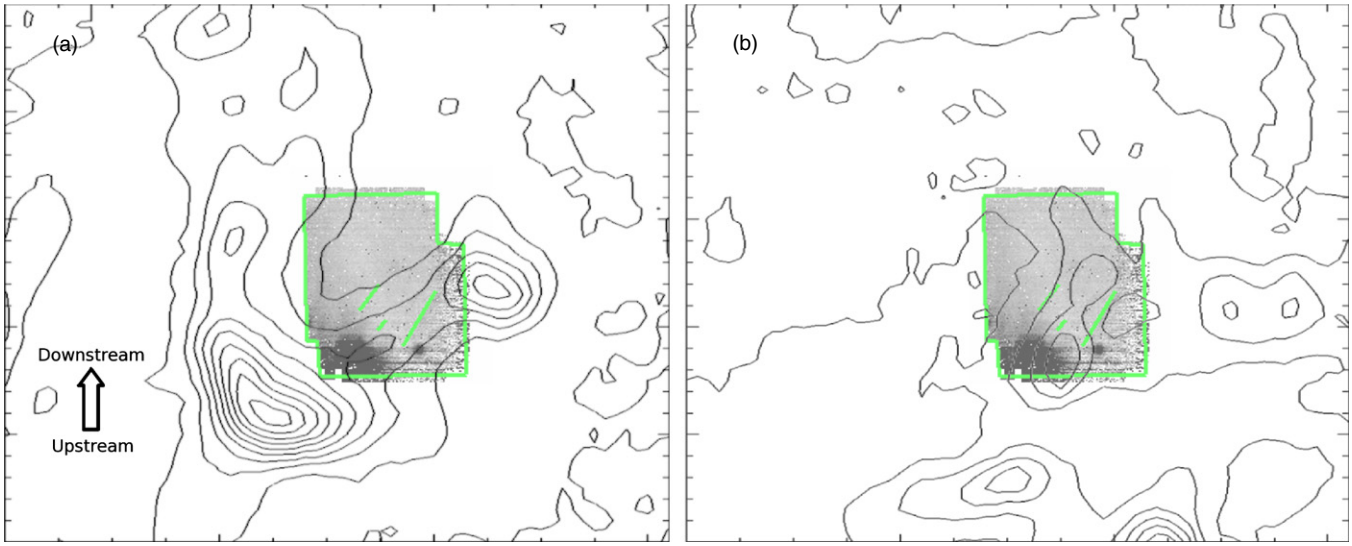

Figure 2. Overlay of the N657-R map in this study with the D1–D3 marks on the H I contour. The size is 5° × 4°; north is up and east to the left. The H I contour is created from the GASS Second Data Release (McClure-Griffiths et al. 2009; Kalberla et al. 2010). (a) The velocities of $-170\,\mathrm{km\,s^{-1}} < v < -250\,\mathrm{km\,s^{-1}}$ are co-added. The contour corresponds to the 2×10^{19} cm^{-2} interval from 2×10^{19} cm^{-2}. (b) The velocities of $-63\,\mathrm{km\,s^{-1}} < v < -15\,\mathrm{km\,s^{-1}}$ are co-added. The contour corresponds to the 1×10^{19} cm^{-2} interval from 3×10^{19} cm^{-2}.

(A color version of this figure is available in the online journal.)

Table 2
Flux-weighted Center of the Hα Emitting Regions

Name	R.A. (J2000)	Decl. (J2000)	l	b
MS IV-D1	23:40:43	−11:09:06	73.3891	−66.9449
MS IV-D2	23:40:13	−11:19:40	72.8502	−66.9864
MS IV-D3	23:39:17	−11:21:00	72.3947	−66.8430

R band, because a residual of subtraction may remain in the N657-R image at the position. Next, we applied a 7 × 7 pixel (10.5 × 10.5 arcsec^2) median filtering to gain S/N. Then the *R*-band image is subtracted from the N657 image and binned into 10 × 10 pixels (15 × 15 arcsec^2). In the image, we defined the boundary as the isophote of 220 mR, which corresponds to 1σ. Above the isophote the regions are ∼2 arcmin wide and are 16, 6, and 29 arcmin long for D1, D2, and D3, respectively. The interval between D1 and D2 is about 12 arcmin, and that between D2 and D3 is also ∼12 arcmin. If the regions lie at MS distance (55 kpc; Putman et al. 2003b), the width of the three Hα regions is 30 pc, the intervals between them are 200 pc each, and the lengths are 100–500 pc.

For photometric analysis, we used the isophote as the boundary and extracted the regions before median filtering. The SB of the Hα regions in the N657–R image is 370 mR on average in 15 arcsec^2, which corresponds to Hα+[N II] brightness of $\sim 2.1 \times 10^{-18}$ erg s^{-1} cm^{-2} arcsec^{-2}. The SB gradient is seen in D1 and D3. The northwest edge is the faintest in SB in D3, and the gradient is about 20 mR arcmin^{-1}. The gradient in D1 has an opposite direction; the SB is the faintest at the southeast edge, rises by 60 mR arcmin^{-1} for 10 arcmin, then gradually get fainter toward northwest. The gradient is not seen in D2.

4. COMPARISON WITH Hα SURVEYS

Our observed field was covered by two Hα surveys. One is SHASSA (Gaustad et al. 2001). The Hα bandwidth (3.2 nm) of SHASSA is comparable to our N657. Finkbeiner (2003) removed stellar contamination from the SHASSA data and calibrated the flux.[9] There are several bright parts in the SHASSA data which overlap D1–D3. However, when we checked the original data of SHASSA, they are not permanent but variable among exposures. We think that the bright parts would be artifacts.

The other survey is WHAM, which covers a velocity range of ∼ ±80 km s^{-1} with respect to the LSR. One of the WHAM beams, $(l, b) = (73.377, -67.054)$, is just on D1 (Haffner et al. 2003). If we average the Hα+[N II] flux of the regions D1–D3 in the 1° aperture of WHAM, it would be observed as a ∼ 5 mR excess, which is too faint to be found in WHAM.

5. COMPARISON WITH H I MAP

We overlap the position of the Hα regions on the H I contour in Figure 2 using the Galactic All-Sky Survey (GASS) Second Data Release (McClure-Griffiths et al. 2009; Kalberla et al. 2010).[10] The regions D1–D3 lie on an overlap of two H I components at $v_{\rm LSR} \sim -210\,\mathrm{km\,s^{-1}}$ and $v_{\rm LSR} \sim -30\,\mathrm{km\,s^{-1}}$. We thus co-add the GASS data over two velocity ranges: −170 to − 250 km s^{-1} as the high velocity component (HVC), and −15 to − 63 km s^{-1} as the low velocity component (LVC).

In the HVC map (Figure 2(a)), an H I cloud with a horseshoe-like morphology is located at $(l, b) = (73.5, -68)$ (Brüns et al. 2005), which is at the southeast of our observed field. The H I cloud is also recognized in the $-211.2\,\mathrm{km\,s^{-1}}$ panel of Figure 6 of Putman et al. (2003b). They mentioned that filaments of the MS appear to merge at several points, and there are dense concentrations of gas at these points. They listed the cloud at $(l, b) = (74, -68)$ as an example of the merging points. The regions D1–D3 are located on this cloud. Spatial correspondence between D1–D3 and the H I cloud suggests that the Hα regions are associated with the MS, and we regard them as candidates of Hα emitting regions of the MS. The H I column density around the Hα regions is (2–6) × 10^{19} cm^{-2} from the contour of Brüns et al. (2005).

[9] http://skymaps.info/
[10] http://www.astro.uni-bonn.de/hisurvey/

In the LVC (Figure 2(b)), there are two clouds around the edge of the filaments, and it is also possible that D1–D3 are associated with the LVC. The H I column density around the Hα regions is (3–6) × 10^{19} cm^{-2}.

6. COLUMN DENSITY OF THE IONIZED GAS

We roughly estimate the column density of the ionized gas. As the typical flux is 370 mR including [N II], we adopt 300 mR for the Hα flux in this section, assuming [N II]/Hα ∼ 0.2 (Ly et al. 2007) for simplicity. The value is a typical one for H II regions, and it would be largely different if the ionization process is different, such as shocks. We assume that the Hα emitting region is a homogeneously distributed, optically thin gas cloud, and is embedded in an isotropic radiation field. For Hα, 1 Rayleigh corresponds to an emission measure (EM) of about 2 cm^{-6} pc (McCullough & Benjamin 2001). Therefore, the EM of D1–D3 is ∼ 0.6 cm^{-6} pc. The EM is written as

$$\mathrm{EM} = \langle n_e^2 \rangle L = 0.6\,\mathrm{cm}^{-6}\,\mathrm{pc}, \quad (2)$$

where n_e is the electron density and L is the mean length of line of sight. The column density is then

$$\sqrt{\langle n_e^2 \rangle} L = 7.6 \times 10^{18} \left(\frac{L}{10\,\mathrm{pc}} \right)^{1/2} \mathrm{cm}^{-2}. \quad (3)$$

It is about 1/2 to 1/8 of H I column density ((2–6) × 10^{19} cm^{-2}), if L = 10 pc.

This rough calculation may overestimate the column density because, in reality, the Hα SB distribution is not homogeneous. In addition, the redshift and the degree of [N II] contamination are unknown.

7. COMPARISON WITH MODEL BY B07

Since WW96 discovered Hα emission from the MS, several hypotheses have been proposed for the ionization mechanism of the Hα emitting gas. A promising theory is the shock-induced model presented by B07. They suggested that the interaction between the fragmented clouds formed in the upstream of MS and the tenuous gas ablated from the upstream clouds would lead to shock ionization at the leading edges of the downstream clouds.

If the northwest cloud in Figure 2(a), which lies in the downstream of the main MS IV cloud at the southeast, is following the main cloud, Hα would be emitted at the leading edge of the northwest cloud according to the B07 model. On the contrary, D1–D3 appear to lie along the H I stream between the northwest and the main clouds. Their straight and almost parallel filamentary morphology do not resemble the Hα distribution predicted by B07. However, note that the widths of D1–D3, ≈30 pc, are smaller than the spatial resolution of the simulations (≈40 pc) of B07. In addition, kiloparsec scale structures of the Hα emission may be lost in this study due to our sky subtraction method (see Section 2). Thus, the spatial resolution mismatch between our observation and the B07 simulation may lead this apparent inconsistency in ionized gas morphology. The Hα regions we detected may be a part of dense ridges, which can be formed by Kelvin–Helmholtz instability at the H I cloud surface, of tenuously extended ionized clouds.

8. POSSIBILITY OF FOSSIL STRÖMGREN TRAIL

The long and straight shape of D1–D3 resembles the Hα filament reported by McCullough & Benjamin (2001, hereafter MB01). The MB01 cloud has a region 20 arcsec wide and 1°.2 long and forks into two segments, with the widest separation at 5 arcmin.

MB01 presented four possible origins for such a cloud: (1) a jet, (2) a filamentary local nebula, (3) a shock-ionized trail, and (4) a Fossil Strömgren Trail (FST), and they concluded their object would be FST. If D1–D3 are local objects, the origin of D1–D3 would be one of the four. Following the discussion by MB01, the faint SB rejects (1), and the straight shape and the intensity gradient along the shape reject (2), and the 2 arcmin width rejects (3) as the D1–D3 origin. And (4), FST by a single star, is difficult, since the gradient has opposite directions in D1 and D3. If D1–D3 are local objects, the possible origin is that they are FSTs of different stars. All three might be made by three different stars or by two stars if D2 is a branch of D1 or D3 like the Y-shaped filament found by MB01.

If D1–D3 are FSTs, we can estimate the distance using Equation (5) of MB01. Putting I $(\mathrm{H}\alpha)_{\mathrm{obs}}$ = 300 mR, width γ = 2 arcmin, and the assumption by MB01 that projection factor p = 1, temperature $T = 10^4$ K, and density n = 1 cm^{-3}, we can estimate that the distance is ∼180 pc. The physical size is 0.1 pc wide and 0.3–1.5 pc long.

9. SUMMARY

We detected three filamentary Hα emitting regions in the MS IV-D field. Their sizes are 2 arcmin wide and 6–30 arcmin long, and the SB of Hα+[N II] is 370 mR on average in the 15 arcsec bin. They are candidates of Hα emitting regions associated with MS IV, although we cannot deny the possibility that they are local objects. If they are at MS distance, the size is 30 pc × 100–500 pc. If they are local objects, FST (McCullough & Benjamin 2001) created by more than two stars is a possible interpretation. Future spectroscopic follow-up will reveal whether they are a part of MS.

We thank the anonymous referee for valuable comments and suggestions. We thank the staff at Kiso Observatory for their kind supports. We thank Christian Brüens, Juergen Kerp, and Peter M. W. Kalberla for important comments and suggestions. We thank Shin-Ichi Ichikawa and Satoshi Kawanomoto for information about data reduction. This study was partly supported by KAKENHI 21540247 and 23244030. This work has made use of the SDSS,[11] NED,[12] SMOKA archive[13] and the computers at ADC NAOJ.

REFERENCES

Abazajian, K. N., Adelman-McCarthy, J. K., Agüeros, M. A., et al. 2009, ApJS, 182, 543
Bertin, E., & Arnouts, S. 1996, A&AS, 117, 393
Bland-Hawthorn, J., & Maloney, P. R. 1999, ApJ, 510, L33
Bland-Hawthorn, J., Sutherland, R., Agertz, O., & Moore, B. 2007, ApJ, 670, L109 (B07)
Brüns, C., Kerp, J., Staveley-Smith, L., et al. 2005, A&A, 432, 45
Finkbeiner, D. P. 2003, ApJS, 146, 407
Fox, A. J., Wakker, B. P., Smoker, J. V., et al. 2010, ApJ, 718, 1046
Gaustad, J. E., McCullough, P. R., Rosing, W., & Van Buren, D. 2001, PASP, 113, 1326
Haffner, L. M., Reynolds, R. J., Tufte, S. L., et al. 2003, ApJS, 149, 405
Itoh, N., Soyano, T., Tarusawa, K., et al. 2001, Publ. Natl. Astron. Obs. Japan, 6, 41

[11] http://cas.sdss.org/
[12] http://nedwww.ipac.caltech.edu/
[13] http://smoka.nao.ac.jp/

Kalberla, P. M. W., McClure-Griffiths, N. M., Pisano, D. J., et al. 2010, A&A, 512, A17
Ly, C., Malkan, M. A., Kashikawa, N., et al. 2007, ApJ, 657, 738
Mathewson, D. S., Cleary, M. N., & Murray, J. D. 1974, ApJ, 190, 291
McCullough, P. R., & Benjamin, R. A. 2001, AJ, 122, 1500
McClure-Griffiths, N. M., Pisano, D. J., Calabretta, M. R., et al. 2009, ApJS, 181, 398
Mink, D. J. 2002, in ASP Conf. Ser. 281, ADASS XI, ed. D. A. Bohlender, D. Durand, & T. H. Handley (San Francisco, CA: ASP), 169
Monet, D. G., Levine, S. E., Canzian, B., et al. 2003, AJ, 125, 984
Putman, M. E., Bland-Hawthorn, J., Veilleux, S., et al. 2003a, ApJ, 597, 948
Putman, M. E., Staveley-Smith, L., Freeman, K. C., Gibson, B. K., & Barnes, D. G. 2003b, ApJ, 586, 170
Raynolds, R. J., Tufte, S. L., Haffner, L. M., Jaehnig, K., & Percival, J. W. 1998, PASA, 15, 14
Schlegel, D. J., Finkbeiner, D. P., & Davis, M. 1998, ApJ, 500, 525
Stanimirorović, S., Hoffman, S., Heiles, C., et al. 2008, ApJ, 680, 276
Weiner, B. J., Vogel, S. N., & Williams, T. B. 2001, in ASP Conf. Ser. 240, Gas and Galaxy Evolution, ed. J. E. Hibbard, M. Rupen, & J. H. van Gorkom (San Francisco, CA: ASP), 515
Weiner, B. J., & Williams, T. B. 1996, AJ, 111, 1156 (WW96)
Yagi, M., Kashikawa, N., Sekiguchi, M., et al. 2002, AJ, 123, 66
Yagi, M., Yoshida, M., Komiyama, Y., et al. 2010, AJ, 140, 1814
Zacharias, N., Monet, D. G., Levine, S. E., et al. 2005, VizieR Online Data Catalog, 1297, 0